I&EC research
Industrial & Engineering Chemistry Research

Article

Cite This: Ind. Eng. Chem. Res. 2018, 57, 11903−11910

pubs.acs.org/IECR

Synergistic Effect of TiO_2−SiO_2 in Ag/Si−Ti Catalyst for the Selective Catalytic Oxidation of Ammonia

Fei Wang,[†,‡] Jinzhu Ma,[†,‡,§] Guangzhi He,[†] Min Chen,[†,‡] Shaoxin Wang,[†] Changbin Zhang,*[,†,‡] and Hong He[†,‡,§]

[†]State Key Joint Laboratory of Environment Simulation and Pollution Control, Research Center for Eco-Environmental Sciences, Chinese Academy of Sciences, Beijing 100085, China

[‡]University of Chinese Academy of Sciences, Beijing 100049, China

[§]Center for Excellence in Regional Atmospheric Environment, Institute of Urban Environment, Chinese Academy of Sciences, Xiamen 361021, China

ABSTRACT: In this study, Ag supported on TiO_2, SiO_2, and SiO_2−TiO_2 catalysts were prepared through the impregnation method and their performance for the selective catalytic oxidation of ammonia (NH_3−SCO) was tested. The results showed that the Ag/SiO_2−TiO_2 (denoted as Ag/Si−Ti) performed at a much higher activity than Ag/TiO_2 and Ag/SiO_2 at low temperature range. Characterization results revealed that SiO_2 possessed a high surface area, but lacked OH groups and acidic sites; TiO_2 possessed abundant OH groups and acidic sites, but the surface area was low. High surface area and abundant OH groups were a benefit for the dispersion of Ag, and acidic sites contributed to the adsorption and activation of ammonia. The synergistic effect compromised the advantages and disadvantages of SiO_2 and TiO_2, which improved the dispersion of Ag, enriched acidic sites of the catalyst and maintained Ag^0 content at an appropriate level, therefore enhanced the NH_3−SCO activity of Ag/Si−Ti catalyst.

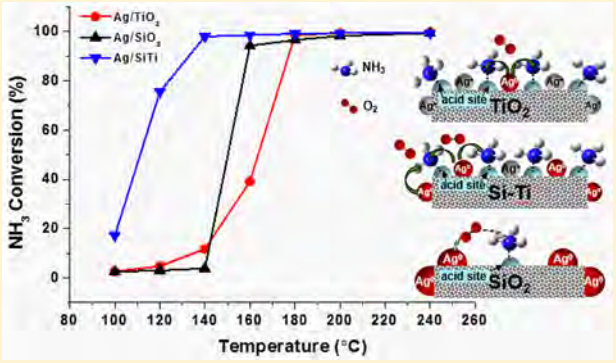

1. INTRODUCTION

Ammonia (NH_3) is a common gas used in agriculture (nitrogen fertilizer), petroleum refining, and deNO_x processes.[1,2] The NH_3 emission from these processes has potential harm to both human health and environment. Especially, it is conducive to the formation of haze in China, according to the latest reports.[1,3−5] Therefore, the controlling of NH_3 emissions is essential.

Various types of techniques have been reported in ammonia elimination, for example, adsorption, biofiltration, catalytic combustion, and catalytic oxidation, etc.[6−8] NH_3−SCO method has distinct advantages for high efficiency and mild reaction condition, which is consequently considered to be a promising method to reduce NH_3 emissions. TiO_2, SiO_2, and Al_2O_3 are the common support materials in NH_3−SCO catalysts. Composite supports, such as SiO_2−TiO_2 and TiO_2−Al_2O_3, were reported to possess the advantages of better redox abilities, higher surface areas, and enhanced acidic sites[9] compared to single-component oxide supports. However, the performance of composite oxide carriers were seldom researched in NH_3−SCO field. In our previous study,[10,11] alumina supported Ag (Ag/Al_2O_3) catalysts were found to possess high NH_3−SCO activity. Therefore, it is worthy of investigating if the SiO_2−TiO_2 support will promote the NH_3−SCO activity of Ag supported catalyst.

In this paper, single and composite carrier supported catalysts Ag/TiO_2, Ag/SiO_2 and Ag/Si−Ti were prepared by impregnation method. The NH_3−SCO activity (NH_3 conversion and N_2 selectivity) of the catalysts were evaluated and compared. Characterizations including BET, XRD, HRTEM, XPS, H_2-TPR, XAFS, NH_3-TPD, and in situ DRIFTS were performed to elucidate the structure−activity relationship of the catalysts. And on this basis, the mechanism of Ag anchoring was also preliminarily revealed.

2. MATERIALS AND METHODS

2.1. Catalysts Preparation. SiO_2 (Aerosil, Sigma-Aldrich) and TiO_2 (Degussa P25) were purchased to prepare the Ag/SiO_2, Ag/TiO_2, and Ag/Si−Ti catalysts. Before that the SiO_2−TiO_2 (Si−Ti) composite support was prepared according to the following steps. First, SiO_2 and TiO_2 powders were blended in deionized water with weight ratio of TiO_2:SiO_2 was 80:20 and stirred for 1 h. Vacuum rotatory evaporator was used for the drying of suspension and then the obtained sample was dehydrated at 105 °C for 12 h. The dried samples were calcinated at 500 °C for 2 h to obtain the SiO_2−TiO_2

Received: May 18, 2018
Revised: August 9, 2018
Accepted: August 13, 2018
Published: August 13, 2018

DOI: 10.1021/acs.iecr.8b02205
Ind. Eng. Chem. Res. 2018, 57, 11903−11910

(Si−Ti) composite support. The Ag/SiO_2, Ag/TiO_2 and Ag/Si−Ti catalysts were prepared through impregnation method, 10 wt % Ag loading was chosen according to our previous studies.[10,11] Typically, same amount of SiO_2, TiO_2 and Si−Ti powder along with deionized water to form suspension, amount of $AgNO_3$ aqueous solution was then introduced and stirred for 3 h. After that, the samples were dehydrated at 120 °C for 6 h and calcinated at 500 °C for 3 h. Finally, the samples were crushed and screened into 40−60 mesh powders.

2.2. Sample Characterization. Quantachrome Quantasorb SI-MP analyzer (Quanta Chrome Instrument Co.) was used to obtain the surface area and pore size distribution of catalysts. The catalysts were outgassed in N_2 flow at 300 °C for 4 h before nitrogen adsorption at −196 °C. The crystalline structure of the samples were detected by XRD (Bruker D8 ADVANCE Diffractometer) with Cu K_α radiation source (λ = 0.15406 nm) at 40 kV and 40 mA. The spectra were collected with 2θ ranging from 10 to 90° with a scan speed of 6° min^{-1}. JEOL JEM 2010 TEM was used to collect HR-TEM images and the acceleration voltage was 200 kV.

XPS was measured on an X-ray photoelectron spectrometer (PHI Quantera, ULVAC-PHI, Inc.) with Al Kα radiation. The binding energies of all the elements were calibrated internally by C 1s (BE = 284.8 eV). XAFS measurements of the Ag−K edge was carried out on the BL14W1 XAFS beamline at the Shanghai Synchrotron Radiation Facility (SSRF) and the PE storage ring was operated at 3.5 GeV with 200 mA. Athena program (contained in IFFEFIT software package) was used to process and analysis the XAFS data.[12] The filtered k^2 weighted $\chi(k)$ was Fourier transforms into R space (k range: 2.2−12.8 $Å^{-1}$). H_2-TPR was measured through Micromeritics AutoChem II 2920 instrument, with a TCD detector continuously monitoring the consumption of H_2. The catalysts (100 mg) were pretreated with 20% O_2/Ar (50 mL·min^{-1}) at 300 °C for 30 min, and then purged in Ar flow for 30 min. After that, 10% H_2/Ar (50 mL·min^{-1}) was introduced into the sample with temperature range from 20 to 700 °C (ramp rate of 10 °C·min^{-1}).

NH_3-TPD spectra was collected on a quadrupole mass spectrometer (MKS Cirrus) by monitoring the signals of NH_3 (m/z = 17). The catalysts (100 mg) were pretreated at 400 °C for 30 min with 20% O_2/N_2 (50 mL·min^{-1}) and exposed to NH_3 for 1 h at 50 °C, and then purged by Ar for 30 min. Finally, the temperature was increased to 400 °C under N_2 atmosphere with the rate of 10 °C·min^{-1}. In situ DRIFTS was recorded on a NEXUS 670-FTIR spectrometer with an MCT/A detector. The samples were pretreated at 500 °C for 30 min with 20 vol % O_2/N_2, and then purged with N_2 to collect the background spectrum. All spectra were collected with a resolution of 4 cm^{-1} and the accumulation of 100 scans.

2.3. Catalytic Activity Test. The NH_3−SCO activity of the catalysts were tested under atmospheric pressure with a fixed-bed reactor (diameter of 4 mm). The total gas flow was 100 mL·min^{-1} with GHSV of 28 000 h^{-1}, containing NH_3 (500 ppm), O_2 (10 vol %) and balance N_2. The concentration of NH_3 and reaction products (NO, NO_2, N_2O) were analyzed by an online FTIR spectrometer equipped with a DTGS detector. NH_3 conversion (X_{NH3}) and N_2 selectivity (S_{N2}) were calculated as follows:·

$$X_{NH3} = 1 - \frac{[NH_3]out}{[NH_3]in} \times 100\% \quad (1)$$

$$S_{N2} = \frac{[NH_3]in - 2[N_2O]out - [NO_2]out - [NO]out}{[NH_3]in} \times 100\% \quad (2)$$

3. RESULTS

3.1. Results of Activity Tests. The performances of Ag/SiO_2, Ag/TiO_2 and Ag/Si−Ti catalysts for the NH_3−SCO were shown in Figure 1. The result showed that Ag/Si−Ti catalyst performed at a much higher catalytic activity than Ag/SiO_2 and Ag/TiO_2. As shown in Figure 1 (A), NH_3 conversion over Ag/Si−Ti started from 100 °C and reached up to 90% at T (temperature) > 130 °C. In contrast, Ag/SiO_2 and Ag/TiO_2 were inactive even at 140 °C and obtained a 90% conversion of NH_3 at 150−170 °C. Thus, it was clear that there existed an obvious synergistic effect between SiO_2 and TiO_2 in Ag/Si−Ti catalyst for NH_3−SCO. The N_2 selectivity (Figure 1 (B))over Ag/Si−Ti was about 60% and the main byproduct was N_2O.

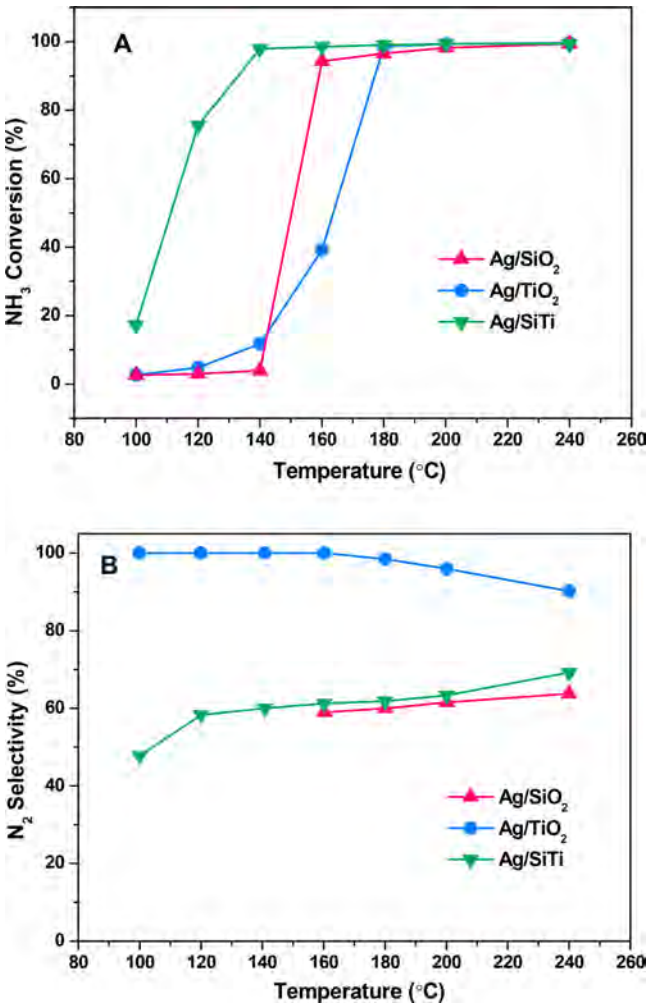

Figure 1. (A) NH_3 conversion (B) N_2 selectivity at different temperatures over Ag/SiO_2, Ag/TiO_2, and Ag/Si−Ti samples.

3.2. Results of Characterization. *3.2.1. Structural Properties.* Table 1 shows the BET surface area (S_{BET}) of Ag/SiO_2, Ag/TiO_2 and Ag/Si−Ti prepared in this study. As can be seen, the S_{BET} of Ag/TiO_2 catalyst was as low as 30.1 m^2/g, while the S_{BET} of Ag/SiO_2 was very high (150.3 m^2/g). The doping SiO_2 into TiO_2 resulted in the higher BET surface

DOI: 10.1021/acs.iecr.8b02205
Ind. Eng. Chem. Res. 2018, 57, 11903−11910

Table 1. BET Surface Area, Pore Volume, and Pore Diameter of the Samples

sample	BET(m^2/g)	pore volume (mL/g)	pore diameter (nm)
Ag/TiO_2	30.1	0.2	3.4
Ag/SiO_2	150.3	1.1	32.4
Ag/Si−Ti	66.5	0.4	21.6

area (66.5 m^2/g) of Ag/Si−Ti catalyst than Ag/TiO_2. The pore volume and pore diameter of Ag/Si−Ti also showed higher values than Ag/TiO_2. Apparently TiO_2 and SiO_2 interacted well.

The XRD patterns for the samples were presented in Figure 2. Diffraction peaks of Ag (111), (200), (220), and (311)

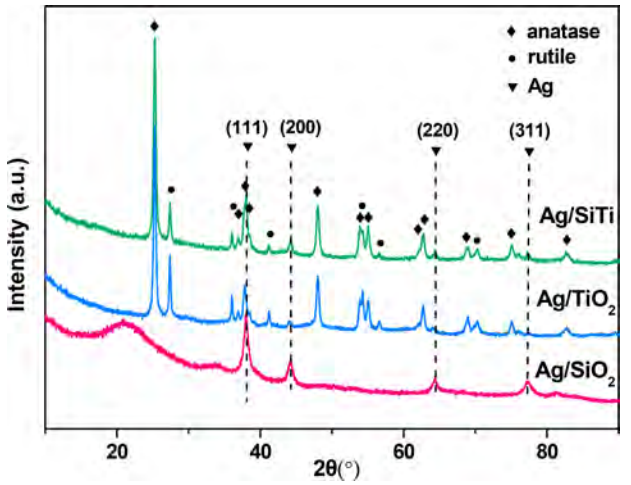

Figure 2. XRD profiles of Ag/SiO_2, Ag/TiO_2, and Ag/Si−Ti catalysts.

lattice planes were observed in all samples.[13] It is obvious that Ag was well-crystallized on Ag/SiO_2, whereas the peaks in Ag/TiO_2 and Ag/Si−Ti were broad and low in intensity. These findings indicated that Ag species were highly dispersed on TiO_2 support possibly due to the strong interaction between metal and support,[14−16] while the interaction between Ag and SiO_2 was so weak that Ag tend to aggregation on SiO_2 during calcination.[15]

The particle-size distribution and the HRTEM images of Ag/SiO_2, Ag/TiO_2, and Ag/Si−Ti catalysts were presented in Figure 3. As can be seen, the Ag particles were uniformly distributed with small size on the TiO_2 and the composite support Si−Ti, while on SiO_2 support, Ag distributed unevenly and formed spherical aggregates with different particle size. The particle size of Ag on Ag/SiO_2, Ag/TiO_2 and Ag/Si−Ti were counted and shown in Figure 3, and the average particle size was 6.4, 4.3, and 4.0 nm, respectively.

3.2.2. Chemical States. In order to acquire the detailed information about the chemical environment and valence state of Ag species over the catalysts, XPS spectra at the Ag 3d core levels were measured and the spectra were presented in Figure 4. The Ag $3d_{5/2}$ core level binding energies of Ag/SiO_2, Ag/TiO_2, and Ag/Si−Ti samples appeared at 368.4, 367.9, and 368.1 eV, respectively. As reported in the literature, the Ag $3d_{5/2}$ at 367.5 eV corresponds to Ag oxide and that 368.3 eV corresponds to metallic Ag.[17] Thus Ag 3d binding energy of Ag/SiO_2 was in accordance with metallic Ag species, which was also in line with XRD diffraction patterns in which metallic Ag peaks were clearly observed. While the Ag $3d_{5/2}$ value of Ag/TiO_2 was close to Ag oxide, which suggested that Ag^+ was the majority in Ag/TiO_2 sample. The Ag $3d_{5/2}$ peak of Ag/Si−Ti (368.1 eV) located at between the corresponding energy of Ag/SiO_2 and Ag/TiO_2. In addition, it can also be observed that the intensity of Ag 3d in Ag/SiO_2 was much weaker than that of Ag/TiO_2 and Ag/Si−Ti due to the aggregation of Ag on Ag/SiO_2.

Figure 5 displayed XAFS data of catalysts (Ag/SiO_2, Ag/TiO_2, and Ag/Si−Ti) and standard samples (Ag-foil and $AgNO_3$). As shown in Figure 5(A), normalized near-edge structure (XANES) of Ag/SiO_2 was similar to Ag-foil, whereas the patterns of Ag/TiO_2 and Ag/Si−Ti were different from the patterns of both Ag-foil and $AgNO_3$. Hence, the Ag/SiO_2 catalyst possessed similar electronic properties and Ag species on SiO_2 was in metallic state,[18] while Ag in Ag/TiO_2 and Ag/Si−Ti existed in the mixture state of Ag^0 and Ag^+. In addition, as presented in Figure 5(B) the normalized first-order derivative peaks of Ag/TiO_2 and Ag/Si−Ti appeared at 25516.8 and 25516.3 eV, respectively. While, the corresponding peaks for the Ag−K edge in Ag foil and $AgNO_3$ were located at 25 514.7 and 25 518.7 eV, respectively. Thus, it can be concluded that more Ag^0 existed in Ag/Si−Ti than in Ag/TiO_2.[19] This speculation was also be confirmed by the XANES fitting result in Table. 2 that the content of Ag^0 in Ag/SiO_2, Ag/TiO_2 and Ag/Si−Ti were 62%, 25% and 33% respectively. This result was in line with XPS.

Fourier transforms of k^2-weighted EXAFS spectra of the catalysts were presented in Figure 5 (C). Consistent with XANES results, intense peaks at 2.67 and 1.64 Å exhibited on all samples, which were attributed to the contiguous Ag−Ag metallic bond[18,20] and Ag−O interactions,[20] respectively. The intensity of the Ag−Ag and Ag−O bonds varied on different samples, and the fitting parameters were given in Table 2. The Ag−Ag coordination number of Ag/SiO_2 sample was much higher than the other two samples, which also revealed more Ag^0 existed in Ag/SiO_2 sample.

In order to investigate the redox ability of Ag/SiO_2, Ag/TiO_2 and Ag/Si−Ti catalysts, H_2-TPR experiments were conducted and the results are presented in Figure 6. Only one obvious peak was observed in Ag/SiO_2 and the H_2 consumption amounts of Ag/SiO_2 was much smaller than Ag/TiO_2 and Ag/Si−Ti samples, which confirms the XPS (Figure 4) and XANES results (Figure 5 A) that Ag was mainly in the form of Ag^0 in Ag/SiO_2 sample. In contrast, there were four main peaks in Ag/TiO_2 with more H_2 consumption, which were located at 66, 139, 343, and 476 °C, respectively. As mentioned,[21] the peak under 100 °C was attributed to the reduction of chemisorbed oxygen on catalysts surface, and the peak near 100 °C was due to the reduction of large Ag_2O clusters; the peaks at around 350 and 450 °C were attributed to the reduction of stable and well dispersed Ag_2O or Ag^+ ions.[21,22] As to Ag/Si−Ti sample, the addition of Si shifted the reduction peak to lower temperatures from 66 °C for Ag/TiO_2 to 58 °C for Ag/Si−Ti. In addition, only three peaks were observed with less H_2 consumption in Ag/Si−Ti indicating that the Ag^0 content and the sample redox ability were improved with the addition of Si.

3.2.3. Surface Acidity. As shown in Figure 7, NH_3-TPD peaks of the samples were deconvoluted into three sub-bands (93 °C, 136 °C, 221 °C), and three bands were attributed to physically adsorbed NH_3, NH_3 bound to weak and strong acid sites,[23] respectively. It is showed that physisorbed NH_3 had a higher proportion on Ag/SiO_2, while the percentage of strong

DOI: 10.1021/acs.iecr.8b02205
Ind. Eng. Chem. Res. 2018, 57, 11903−11910

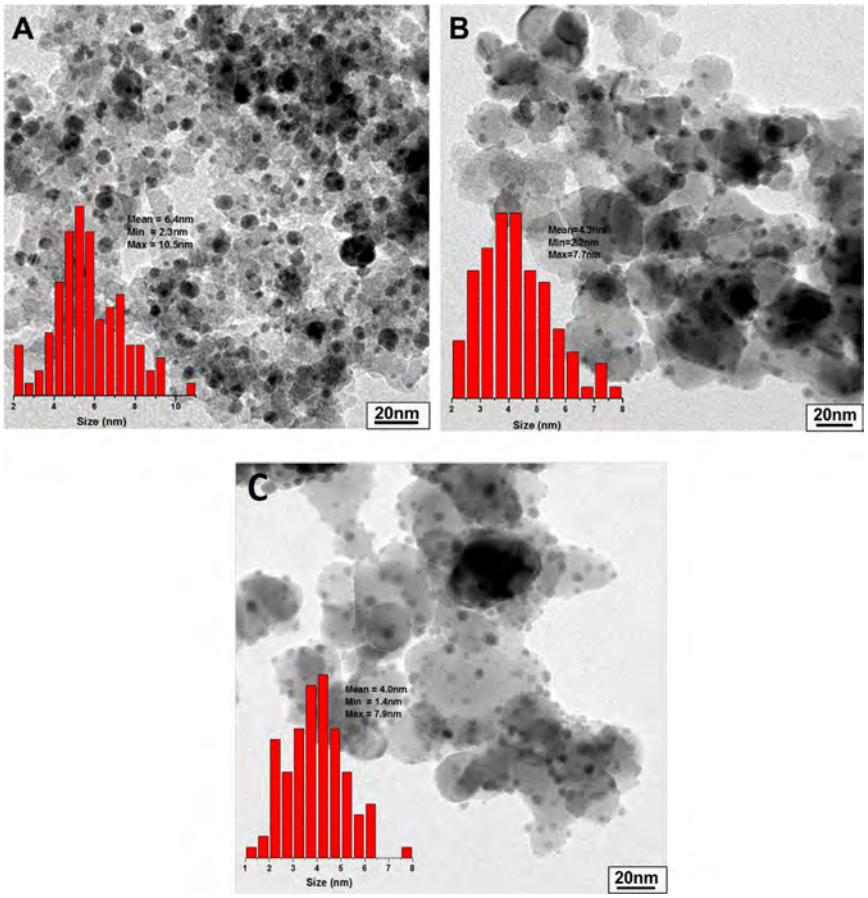

Figure 3. HRTEM of (A) Ag/SiO_2, (B) Ag/TiO_2, and (C) Ag/Si−Ti catalysts.

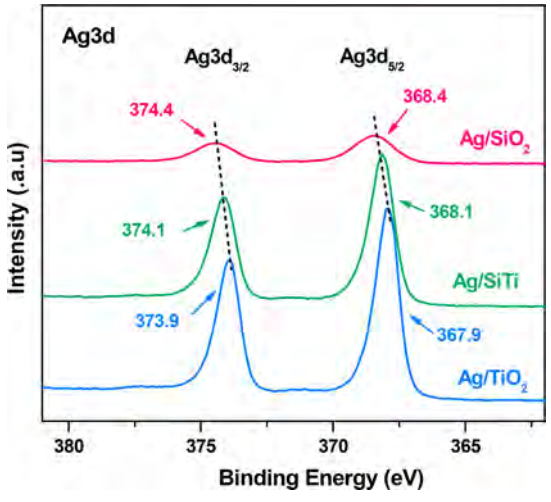

Figure 4. Ag 3d XPS spectra of Ag/SiO_2, Ag/TiO_2 and Ag/Si−Ti.

acidic sites were higher in Ag/TiO_2. Moreover, the addition of SiO_2 to TiO_2 increased the amount of both weak and strong acidic sites. Ag/Si−Ti sample contained much higher surface density of acidic sites, which was beneficial for the adsorption and activation of NH_3.[24−26]

We further checked the difference of acidic sites over SiO_2, TiO_2 and Si−Ti supports through in situ DRIFTS of NH_3 adsorption. It can be observed in Figure 8 A that the adsorption strength of NH_3 was very weak and it was almost disappeared after N_2 purging on SiO_2 support, thus NH_3 was mainly in the form of physical absorption on SiO_2 support. As for TiO_2 and Si−Ti supports in Figure 8B, C, the change of NH_3 adsorption strength was not obvious after N_2 purging. The stable states of NH_3 adsorption on SiO_2, TiO_2 and Si−Ti supports after N_2 purging were compared and presented in Figure 8D. The bands at 3100−3400 cm^{-1} were assigned to the stretching vibration of the N−H bonds in NH_3,[23,27] bands corresponding to Brønsted acidic sites (1436 cm^{-1}) and Lewis acidic sites (1595, 1542, 1242, and 1163 cm^{-1})[23,27] were also detected on TiO_2 and Si−Ti supports. The negative bands at 3400−4000 cm^{-1} were assigned to the consumption of surface hydroxyl groups. It can be seen that SiO_2 had neither acidic sites nor OH groups. Thus, we can conclude both of Brønsted and Lewis acidic sites are significant for NH_3−SCO.

3.2.4. Silver Anchoring. It was reported that metals can be anchored on support through reaction between metal ions and surface hydroxyl groups on the support.[28−30] In order to confirm the dependency of OH and Ag anchoring, the NH_3 adsorption in situ DRIFTS analysis was conducted over Ag/Si−Ti catalysts with different Ag loadings. As shown in Figure 9 A, the intensity of the OH groups decreased rapidly when Ag was added. The hydroxyl peak areas were then calculated by integrating and the correlation between Ag content and hydroxyl peak area was then fitted in Figure 9B. It was clear that OH content correlated strongly with Ag loadings that the correlation coefficients (r^2) above 0.92. These results proved that Ag was anchored on supports surface through the consumption of OH groups.

DOI: 10.1021/acs.iecr.8b02205
Ind. Eng. Chem. Res. 2018, 57, 11903−11910

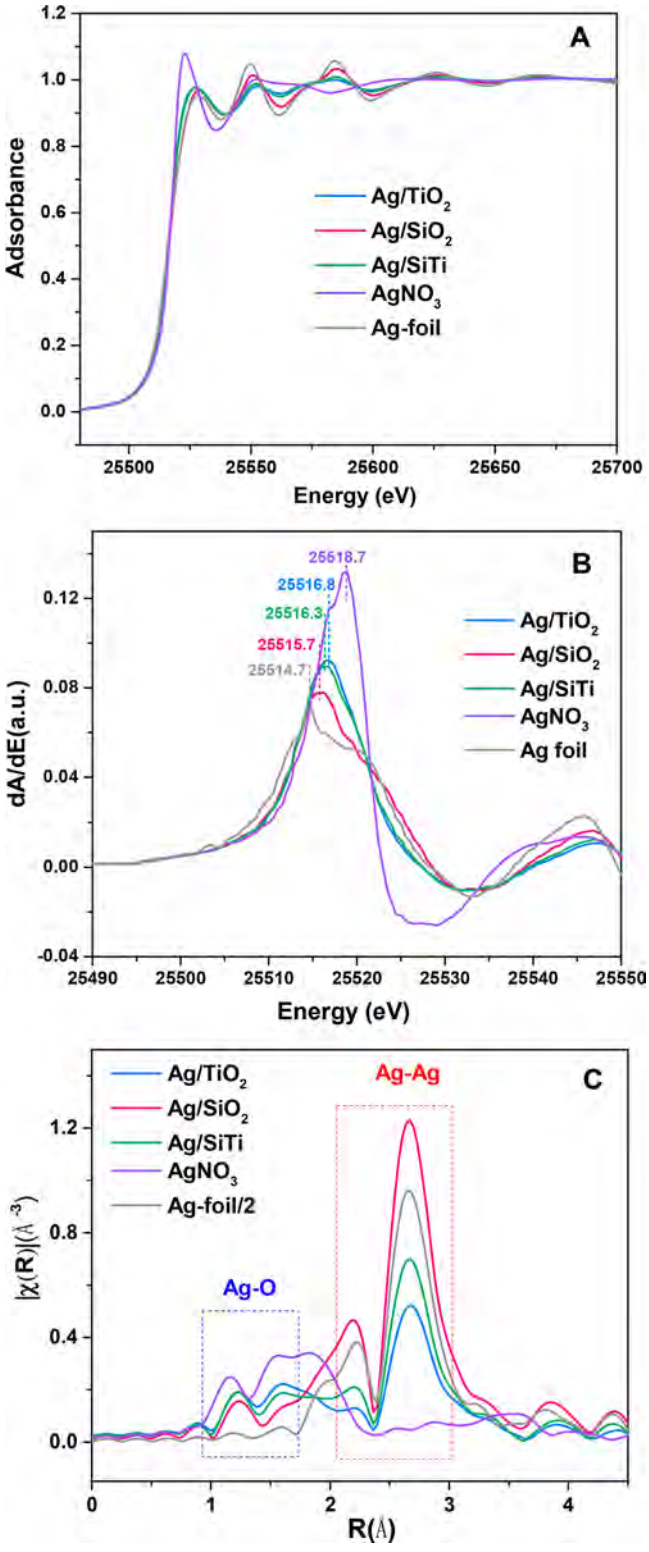

Figure 5. Ag−K edge XAFS spectra, (A) Normalized near-edge structure (XANES), (B) first-order derivatives, (C) k^2 weighted EXAFS spectra (Fourier transform k range 2.2−12.8 Å^{-1}) of catalysts and standard samples

4. DISCUSSION

Ag/TiO_2, Ag/SiO_2, and Ag/Si−Ti catalysts were prepared and the NH_3−SCO activity were tested in this study. The results showed that Ag/Si−Ti possessed a higher low-temperature NH_3−SCO activity (T_{90} = 130 °C) than Ag/TiO_2 (T_{90} = 150

Table 2. Fitting Results of Ag−K XANES and EXAFS

	Ag−K XANES		Ag−K EXAFS				
sample	Ag^0 (%)	Ag^+ (%)	shell	CN[a]	R[b] (Å)	σ^{2c} (10^{-3} Å^2)	R factor (%)
Ag/SiO_2	62	38	Ag−O	0.8 ± 0.3	2.17	11.4	0.17
			$Ag-Ag_1$	6.8 ± 0.9	2.86	9.6	
			$Ag-Ag_2$	9.7 ± 1.7	2.92	56.6	
Ag/TiO_2	25	75	Ag−O	2.1 ± 0.3	2.25	16.7	0.37
			$Ag-Ag_1$	3.5 ± 1.5	2.86	10.9	
			$Ag-Ag_2$	2.7 ± 0.4	3.12	32.8	
Ag/Si−Ti	33	67	Ag−O	1.7 ± 0.3	2.22	15.2	0.33
			$Ag-Ag_1$	4.4 ± 1.2	2.86	10.3	
			$Ag-Ag_2$	2.9 ± 0.9	3.12	35.6	

[a]CN: coordination number. [b]R: bond distance. [c]σ: Debye−Waller factor.

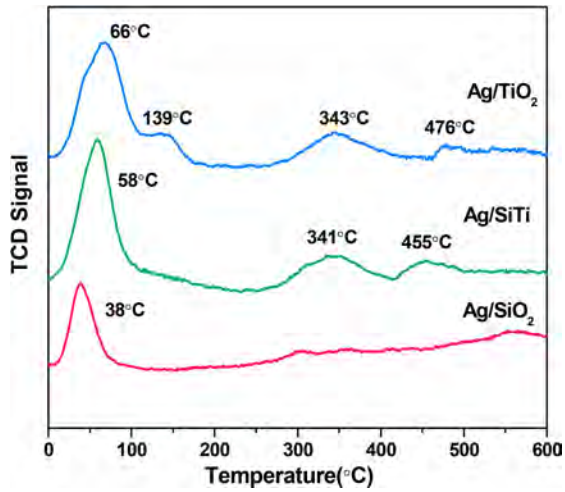

Figure 6. H_2-TPR profiles of Ag/TiO_2, Ag/SiO_2, and Ag/Si−Ti catalysts.

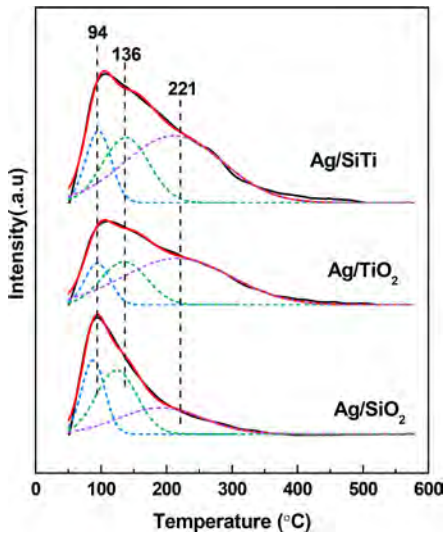

Figure 7. TPD profiles of NH_3 from Ag/TiO_2, Ag/SiO_2, and Ag/Si−Ti catalysts.

DOI: 10.1021/acs.iecr.8b02205
Ind. Eng. Chem. Res. 2018, 57, 11903−11910

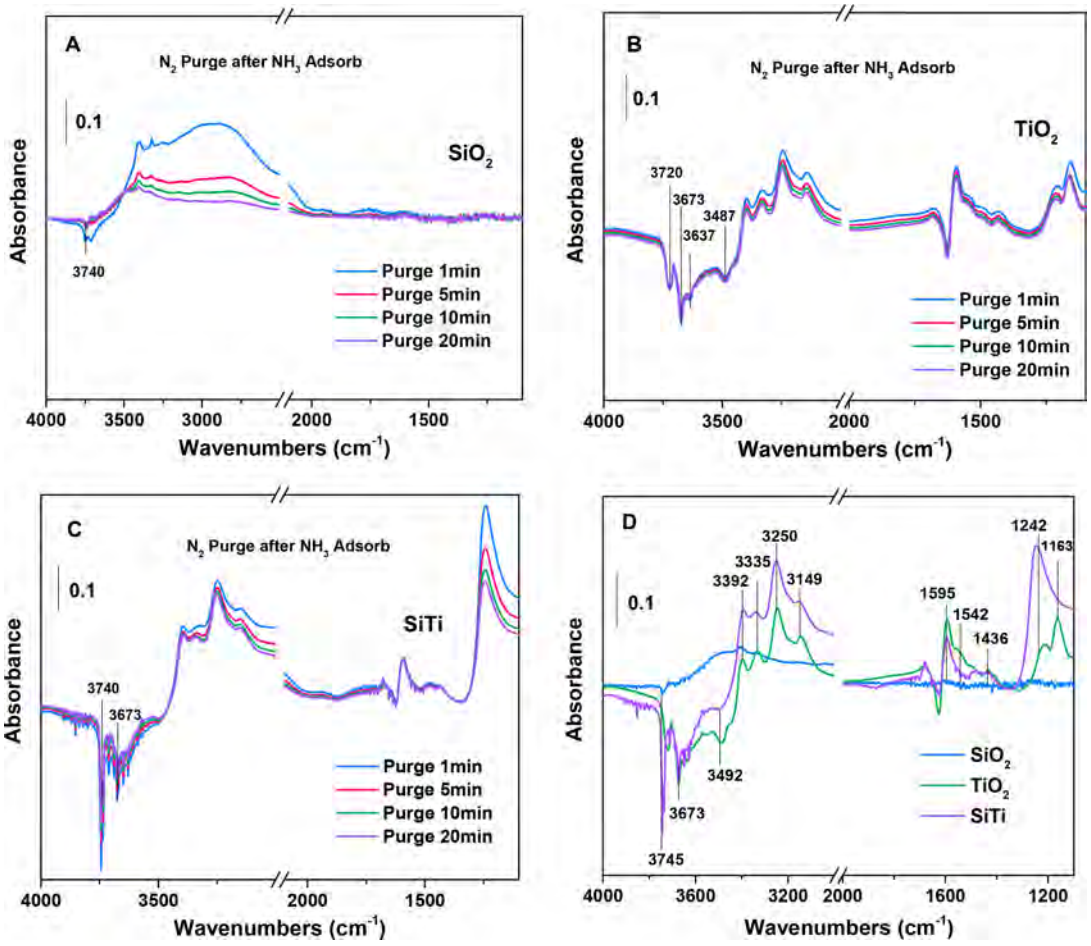

Figure 8. In situ DRIFTS results of N_2 purge after NH_3 adsorption over (A) SiO_2, (B) TiO_2, (C) Si−Ti supports, and (D) comparison of the stable states after N_2 purge at room temperature.

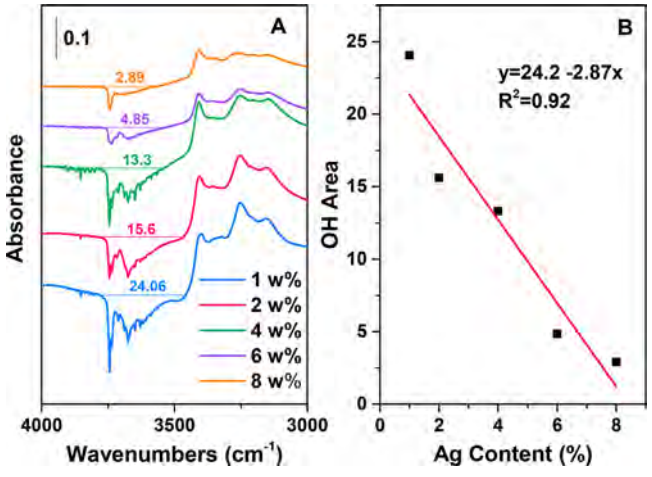

Figure 9. in situ DRIFTS with NH_3 as the probe molecule of hydroxyl content over Ag/Si−Ti catalysts with different Ag loadings (A), linear fitting result of Ag content and hydroxyl peak area (B).

°C) and Ag/SiO_2 (T_{90} = 170 °C), indicating the existence of synergistic effect between SiO_2 and TiO_2 in Ag/Si−Ti catalyst.

It was reported before[28,29] and confirmed in this article that metals were anchored on the support through reaction between metal ions and surface hydroxyl groups on the carrier. Characterization results presented that the BET surface area and average pore diameter of SiO_2 support were huge. Since there is no insufficient OH groups on SiO_2 for Ag anchor, Ag species aggregated into large Ag^0 particles. Metallic Ag was reported to possess higher redox performance,[10] which was also confirmed by the H_2-TPR results that the reduction temperature of Ag/SiO_2 was the lowest. The BET surface area of TiO_2 support was small but there were abundant OH groups, which provided the anchor sites for Ag species, therefore the Ag dispersion on TiO_2 was high. The strong anchoring strength made Ag species tend to oxidation state. Thus, the redox ability of Ag/TiO_2 was relatively poor as performed through the H_2-TPR results. In addition, the surface acidity of Ag/TiO_2 catalyst was high because of the abundant acidic sites of TiO_2 support. As to the composite support SiO_2−TiO_2, the doping of SiO_2 compromised the surface area of SiO_2 and TiO_2 supports, and the synergistic effect enhanced the content of OH groups and acidic sites. The abundant OH groups were benefit for the dispersion of Ag on Si−Ti support and high concentration of acidic sites can conduce to the adsorption and activation of NH_3. According to the literatures, both of Brønsted and Lewis acidic sites are important but they may play the different roles in NH_3−SCO reaction.[24−26] Our recent research also find that Lewis acidic sites can contribute to the dissociation of NH_3, whereas NH_4^+ adsorbed on Brønsted sites are more reactive with O_2. In addition, characterization results also revealed that Ag species in Ag/Si−Ti existed in the mixture state of Ag^0 and Ag^+ and more Ag^0 existed in Ag/Si−Ti than in Ag/TiO_2. We come to the

DOI: 10.1021/acs.iecr.8b02205
Ind. Eng. Chem. Res. 2018, 57, 11903−11910

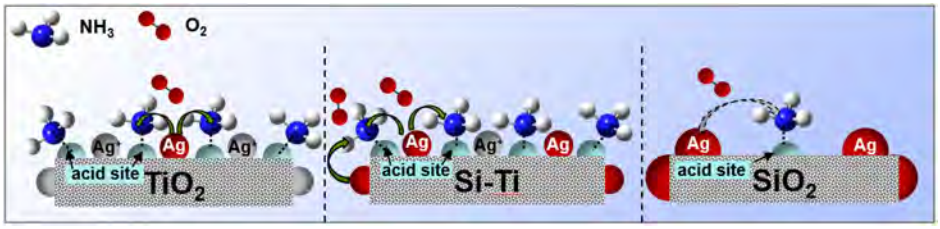

Figure 10. Schematic drawings of the possible process of NH_3 adsorption and activation over the surface of Ag/SiO_2, Ag/TiO_2, and Ag/Si−Ti catalysts.

conclusion that the doping of SiO_2 weakened the anchoring strength of Ag and made it more easily to decompose during calcination into metallic Ag. Since the Ag^0 species are much more active for O_2 activation, high Ag content is also beneficial to the overoxidation of NH_3. In addition, our recent work[11] shows that Ag^0 can contribute to the dissociation of NH_3 to N_2^-, and thus N_2O could be easily generated in the reaction between O_2 and N_2^-. Therefore, although the high Ag^0 content in Ag/Si−Ti catalyst enhanced the NH_3 conversion, it also led to the low N_2 selectivity.

Thus, we can conclude that Ag/SiO_2 catalyst possessed high content of Ag^0 as well as high redox ability. However, the lack of OH groups led to the aggregation of Ag into large particles, meanwhile the insufficient of acidic site limited the adsorption and activation of NH_3. Ag/TiO_2 catalyst possessed abundant OH groups to anchor Ag and the acidic sites was also plentiful. While the strong anchoring strength prompt Ag species to show oxidation state and thus the redox ability of Ag/TiO_2 was relatively poor. What's more, the small surface area of Ag/TiO_2 also limited the NH_3−SCO activity. The defects of Ag/SiO_2 and Ag/TiO_2 were improved through the composition of SiO_2 and TiO_2 supports. Synergistic effect enhanced the dispersion of Ag and content of acidic sites as well as maintained Ag^0 content at a certain level. Therefore, high dispersion of Ag, appropriate content of Ag^0 and abundant acidic sites were crucial factors for NH_3−SCO activity. The features of the three catalysts and the corresponding impact mechanisms for the process of NH_3 adsorption and activation during NH_3−SCO were drawn in Figure 10.

5. CONCLUSIONS

The NH_3−SCO activity of Ag/Si−Ti was higher (T_{90} = 130 °C) than Ag/TiO_2 (T_{90} = 150 °C) and Ag/SiO_2 (T_{90} = 170 °C) at low temperatures. Characterization results indicated that Ag dispersion, Ag species state and surface acidity were crucial factors for NH_3−SCO activity. It was revealed that OH content correlated strongly with Ag loadings and Ag was anchored through the consumption of OH groups. The composition of SiO_2 and TiO_2 enhanced the content of OH groups, which provided the anchoring sites for Ag and thus improved the dispersion of Ag. The synergistic effect also improved the content of acidic sites and maintained Ag^0 content at an appropriate level. Finally, well-dispersed Ag with appropriate Ag^0 content along with abundant acidic sites improved the NH_3−SCO activity of Ag/Si−Ti catalyst.

AUTHOR INFORMATION

Corresponding Author

*E-mail: cbzhang@rcees.ac.cn.

ORCID

Fei Wang: 0000-0002-4364-9956

Jinzhu Ma: 0000-0003-1878-0669

Guangzhi He: 0000-0003-1770-3522

Changbin Zhang: 0000-0003-2124-0620

Notes

The authors declare no competing financial interest.

ACKNOWLEDGMENTS

This work was financially supported by the National Key R&D Program of China (2017YFC0211802, 2017YFC0211101), the National Natural Science Foundation of China (21577159).

REFERENCES

(1) Pan, Y.; Tian, S.; Liu, D.; Fang, Y.; Zhu, X.; Zhang, Q.; Zheng, B.; Michalski, G.; Wang, Y. Fossil Fuel Combustion-Related Emissions Dominate Atmospheric Ammonia Sources During Severe Haze Episodes: Evidence from ^{15}N-Stable Isotope in Size-Resolved Aerosol Ammonium. *Environ. Sci. Technol.* **2016**, *50*, 8049.

(2) Li, P.; Zhang, R.; Liu, N.; Royer, S. Efficiency of Cu and Pd Substitution in Fe-Based Perovskites to Promote N_2 Formation During NH_3 Selective Catalytic Oxidation (NH_3-SCO). *Appl. Catal., B* **2017**, *203*, 174.

(3) Turšič, J.; Berner, A.; Podkrajšek, B.; Grgić, I. Influence of Ammonia on Sulfate Formation under Haze Conditions. *Atmos. Environ.* **2004**, *38*, 2789.

(4) Wang, G.; Zhang, R.; Gomez, M. E.; Yang, L.; Levy Zamora, M.; Hu, M.; Lin, Y.; Peng, J.; Guo, S.; Meng, J.; Li, J.; Cheng, C.; Hu, T.; Ren, Y.; Wang, Y.; Gao, J.; Cao, J.; An, Z.; Zhou, W.; Li, G.; Wang, J.; Tian, P.; Marrero-Ortiz, W.; Secrest, J.; Du, Z.; Zheng, J.; Shang, D.; Zeng, L.; Shao, M.; Wang, W.; Huang, Y.; Wang, Y.; Zhu, Y.; Li, Y.; Hu, J.; Pan, B.; Cai, L.; Cheng, Y.; Ji, Y.; Zhang, F.; Rosenfeld, D.; Liss, P. S.; Duce, R. A.; Kolb, C. E.; Molina, M. J. Persistent Sulfate Formation from London Fog to Chinese Haze. *Proc. Natl. Acad. Sci. U. S. A.* **2016**, *113*, 13630.

(5) Chu, B.; Zhang, X.; Liu, Y.; He, H.; Sun, Y.; Jiang, J.; Li, J.; Hao, J. Synergetic Formation of Secondary Inorganic and Organic Aerosol: Effect of SO_2 and NH_3 on Particle Formation and Growth. *Atmos. Chem. Phys.* **2016**, *16*, 14219.

(6) Chung, Y.; Huang, C.; Liu, C. H.; Bai, H. Biotreatment of Hydrogen Sulfide- and Ammonia-Containing Waste Gases by Fluidized Bed Bioreactor. *J. Air Waste Manage. Assoc.* **2001**, *51*, 163.

(7) Burch, R.; Southward, B. W. L. The Nature of the Active Metal Surface of Catalysts for the Clean Combustion of Biogas Containing Ammonia. *J. Catal.* **2001**, *198*, 286.

(8) Huang, T. L.; Cliffe, K. R.; Macinnes, J. M. The Removal of Ammonia from Water by a Hydrophobic Catalyst. *Environ. Sci. Technol.* **2000**, *34*, 4804.

(9) Liu, C.; Chen, L.; Li, J.; Ma, L.; Arandiyan, H.; Du, Y.; Xu, J.; Hao, J. Enhancement of Activity and Sulfur Resistance of CeO_2 Supported on TiO_2-SiO_2 for the Selective Catalytic Reduction of NO by NO_3. *Environ. Sci. Technol.* **2012**, *46*, 6182.

(10) Zhang, L.; Zhang, C.; He, H. The Role of Silver Species on Ag/Al_2O_3 Catalysts for the Selective Catalytic Oxidation of Ammonia to Nitrogen. *J. Catal.* **2009**, *261*, 101.

DOI: 10.1021/acs.iecr.8b02205
Ind. Eng. Chem. Res. 2018, 57, 11903−11910

(11) Wang, F.; Ma, J.; He, G.; Chen, M.; Zhang, C.; He, H. Nanosize Effect of Al_2O_3 in Ag/Al_2O_3 Catalyst for the Selective Catalytic Oxidation of Ammonia. *ACS Catal.* **2018**, *8*, 2670.
(12) Newville, M. Ifeffit: Interactive XAFS Analysis and FEFF Fitting. *J. Synchrotron Radiat.* **2001**, *8*, 322.
(13) Luo, M.; Yuan, X.; Zheng, X. Catalyst Characterization and Activity of Ag−Mn, Ag−Co and Ag−Ce Composite Oxides for Oxidation of Volatile Organic Compounds. *Appl. Catal., A* **1998**, *175*, 121.
(14) Grünert, W.; Brückner, A.; Hofmeister, H.; Claus, P. Structural Properties of $AgTiO_2$ Catalysts for Acrolein Hydrogenation. *J. Phys. Chem. B* **2004**, *108*, 5709.
(15) Riva, R.; Miessner, H.; Vitali, R.; Piero, G. D. Metal−Support Interaction in Co/SiO_2 and Co/TiO_2. *Appl. Catal., A* **2000**, *196*, 111.
(16) Li, Y.; Zhang, C.; He, H.; Zhang, J.; Chen, M. Influence of Alkali Metals on Pd/TiO_2 Catalysts for Catalytic Oxidation of Formaldehyde at Room Temperature. *Catal. Sci. Technol.* **2016**, *6*, 2289.
(17) Sumesh, E.; Bootharaju, M. S.; Anshup; Pradeep, T. A Practical Silver Nanoparticle-Based Adsorbent for the Removal of Hg^{2+} from Water. *J. Hazard. Mater.* **2011**, *189*, 450.
(18) Verma, P.; Yuan, K.; Kuwahara, Y.; Mori, K.; Yamashita, H. Enhancement of Plasmonic Activity by Pt/Ag Bimetallic Nanocatalyst Supported on Mesoporous Silica in the Hydrogen Production from Hydrogen Storage. *Appl. Catal., B* **2018**, *223*, 10.
(19) Deng, H.; Yu, Y.; Liu, F.; Ma, J.; Zhang, Y.; He, H. Nature of Ag Species on $Ag/\gamma\text{-}Al_2O_3$: A Combined Experimental and Theoretical Study. *ACS Catal.* **2014**, *4*, 2776.
(20) Zhou, W.; Li, T.; Wang, J.; Qu, Y.; Pan, K.; Xie, Y.; Tian, G.; Wang, L.; Ren, Z.; Jiang, B.; Fu, H. Composites of Small Ag Clusters Confined in the Channels of Well-Ordered Mesoporous Anatase TiO_2 and Their Excellent Solar-Light-Driven Photocatalytic Performance. *Nano Res.* **2014**, *7*, 731.
(21) Bethke, K. A.; Kung, H. H. Supported Ag Catalysts for the Lean Reduction of NO with C_3H_6. *J. Catal.* **1997**, *172*, 93.
(22) Son, I. H.; Kim, M. C.; Koh, H. L.; Kim, K.-L. On the Promotion of $Ag/\gamma\text{-}Al_2O_3$ by Cs for the SCR of NO by C_3H_6. *Catal. Lett.* **2001**, *75*, 3.
(23) Peng, Y.; Liu, C.; Zhang, X.; Li, J. The Effect of SiO_2 on a Novel CeO_2-WO_3/TiO_2 Catalyst for the Selective Catalytic Reduction of No with NH_3. *Appl. Catal., B* **2013**, *140−141*, 276.
(24) Macina, D.; Opioła, A.; Rutkowska, M.; Basąg, S.; Piwowarska, Z.; Michalik, M.; Chmielarz, L. Mesoporous Silica Materials Modified with Aggregated Transition Metal Species (Cr, Fe and Cr-Fe) in the Role of Catalysts for Selective Catalytic Oxidation of Ammonia to Dinitrogen. *Mater. Chem. Phys.* **2017**, *187*, 60.
(25) Xu, L.; Wang, C.; Chang, H.; Wu, Q.; Zhang, T.; Li, J. New Insight into SO_2 Poisoning and Regeneration of $CeO_2\text{-}WO_3/TiO_2$ and $V_2O_5\text{-}WO_3/TiO_2$ Catalysts for Low-Temperature NH_3-SCR. *Environ. Sci. Technol.* **2018**, *52*, 7064.
(26) Zhang, L.; He, H. Mechanism of Selective Catalytic Oxidation of Ammonia to Nitrogen over Ag/Al_2O_3. *J. Catal.* **2009**, *268*, 18.
(27) Hadjiivanov, K. Ft-Ir Spectroscopic Study of NH_3 and Co Adsorption and Coadsorption on TiO_2 (Anatase). *Z. Phys. Chem.* **1994**, *187*, 281.
(28) Jacobsen, C. J. H.; Topsøe, N. Y.; Topsøe, H.; Kellberg, L.; Jakobsen, H. J. Quantitative ^1H MAS NMR Studies of Structurally Different OH Surface Groups on $\eta\text{-}Al_2O_3$ and $Mo/\eta\text{-}Al_2O_3$ Catalysts. *J. Catal.* **1995**, *154*, 65.
(29) Kwak, J. H.; Hu, J.; Mei, D.; Yi, C.-W.; Kim, D. H.; Peden, C. H. F.; Allard, L. F.; Szanyi, J. Coordinatively Unsaturated Al^{3+} Centers as Binding Sites for Active Catalyst Phases of Platinum on $\gamma\text{-}Al_2O_3$. *Science* **2009**, *325*, 1670.
(30) Dutov, V. V.; Mamontov, G. V.; Zaikovskii, V. I.; Liotta, L. F.; Vodyankina, O. V. Low-Temperature CO Oxidation over Ag/SiO_2 Catalysts: Effect of OH/Ag Ratio. *Appl. Catal., B* **2018**, *221*, 598.

DOI: 10.1021/acs.iecr.8b02205
Ind. Eng. Chem. Res. 2018, 57, 11903−11910